湖南大学学报（自然科学版）
Journal of Hunan University (Natural Sciences)

第 50 卷 第 10 期
2023 年 10 月

Available online at http://jonuns.com/index.php/journal/index

Vol. 50 No. 10
October 2023

Open Access Article

https://doi.org/10.55463/issn.1674-2974.50.10.8

Complementary Data Regularization for Nonlinear Matrix-Valued Image Denoising

Muzaffar Bashir Arain[1]*, Khuda Bux Amur[1], Rahim Bux Khokhar[2], Memoona Pirzada[3], Izhar Ali Amur[4], Sanaullah Dehraj[1]

[1] Department of Mathematics and Statistics, Quaid-e-Awam University of Engineering, Science & Technology, Nawabshah, 67480, Sindh, Pakistan

[2] Basic Science and Related Studies, MUET, Jamshoro, Sindh, Pakistan

[3] Mathematics Department, Dawood University of Engineering and Technology, Karachi, Sindh, Pakistan

[4] Department of General Faculty, Shaheed Benazir Bhutto University, Shaheed Benazirabad, Sindh, Pakistan

* Corresponding author: muzaffararain@quest.edu.pk

Received: July 19, 2023 / Revised: August 14, 2023 / Accepted: September 12, 2023 / Published: October 31, 2023

Abstract: In this study, we present some findings from applying a complementary data regularization approach to a nonlinear image denoising model. The proposed method uses optimizing non-quadratic energy functionals with normalized data terms. This study aims to develop an image denoising technique that combines well-known robust diffusivity coefficients such as total variation regularization with normalized data term known as complementary data regularization. We apply our modified mathematical approach to the matrix-valued images, a challenging computational task. The primary purpose of the complementary regularization idea of data terms is to create a compatible connection and a reliable balance between diffusion and data terms. The standard finite difference scheme has been considered as a discretization method for the numerical solution of the partial differential equation obtained from the variational optimization of the modified energy function. The performance of the proposed model is demonstrated through numerous numerical experiments in terms of image quality analysis and computational time. Comparison of the results with some well-known classical methods such as Perona–Malik, total variation, and non-local mean methods in the literature is the heart of this work.

Keywords: image denoising, isotropic diffusion, complementary regularization, variational optimization.

非線性矩陣值影像去雜訊的互補資料正規化

摘要：在本研究中，我們提出了將互補資料正規化方法應用於非線性影像去噪模型的一些發現。所提出的方法使用具有歸一化資料項的最佳化非二次能量泛函。本研究旨在開發一種影像去雜訊技術，該技術將眾所周知的穩健擴散係數（例如全變分正則化）與稱為互補資料正則化的歸一化資料項相結合。我們將修改後的數學方法應用於矩陣值影像，這是一項具有挑戰性的計算任務。資料項的互補正則化想法的主要目的是在擴散項和資料項之間創建相容的連接和可靠的平衡。標準有限差分格式被認為是透過修正能量函數的變分優化所獲得的偏微分方程數值解的離散化方法。透過影像品質分析和計算時間方面的大量數值實驗證明了所提出模型的性能。將結果與文獻中一些著名的經典方法（例如佩羅納馬利克、全變異和非

局部均值方法）进行比較是這項工作的核心。

关键词：影像去噪、各向同性擴散、互補正規化、變分優化。

1. Introduction

In acquiring, transmitting, and storing images, noise appears as a typical phenomenon. For instance, random noise of varying intensities will be added to the obtained image if the imaging sensor's surface has damaged pixels that cannot register incident light. Examples of noise models include salt and pepper [1], Gaussian and Poisson [2], shot [3], and speckle [4, 5]. In nature, they can be additive (noise added to the original image) or multiplicative (noise multiplied to the initial image). Denoised images are better suited for later image processing, analysis, and comprehension. As a result, image denoising is a critical component of image processing and has been the subject of extensive research [4, 6–12]. The variational approach in imaging technologies is a modern approach that optimizes energy functions consisting of regularization and data terms [13–17]. In mathematical imaging techniques, it is usual practice that researchers use gray values as data [12–22], which is a simple computational task, whereas image denoising specifically for matrix-valued (color) images is an essential aspect of the computation. The optimization of the variational model imaging methods yields partial differential equations in the form of anisotropic and isotropic diffusion equations [13, 19, 22–24]. The partial differential equations (PDE's) based filters are broadly used in mathematical image processing techniques for image reconstruction, enhancement, and other applications, such as optical flow and stereo vision [25, 26]. Therefore, to overcome these challenges, scholars have proposed existing image denoising/enhancement methods, including total variation image regularization [13–17], diffusion models such as [19–21, 27–29], wavelet thresholding such as [30–32], bilateral filtering, non-local means filtering [33, 34], and block matching and 3D filtering [35, 36]. Removing noise while preserving edges and other important information A great deal of research has gone into understanding the models. Recently, among the image denoising techniques, PDEs and variational methods have become popular methods for image denoising [12–17, 19–22]. The best known is the total variation model proposed in [13, 22]. Usually, nonlinear variational models are applied to preserve important information, such as edges of imaging processes. Although this nonlinear second-order PDE is a helpful agent to preserve edges, the staircase effects are a common issue in the smooth region of the image. Numerous mathematical models have been proposed to overcome the staircase effects. Since denoising is an ill-posed problem, the research community is still working to achieve the desirable accuracy of the computed solution as the denoised image. A novel approach in [25], from the modeling point of view, was proposed as a modification in quadratic regularization for the optic flow problem as normalization of the data term. This novel idea is known as complementary data regularization. The main goal was to regularize the data and smoothness terms simultaneously, which is a novel idea for estimating optical flow from a sequence of images. Adaptive control of regularization (complimentary image motion problem) based on a posteriori error estimation [26] for a variational optic flow model, which was designed using a complementary approach [25] and successfully applied. The idea is based on optimizing a quadratic function in L^2 (Ω) and proposes image-driven diffusivity with complementary regularization for image-denoising problems [37]. The authors of [25] propose a similar strategy for other applications. Under the above suggestions, we combine the regularized version of total variation (TV) smoothing with complimentary data regularization for color image restoration. The main contributions of this work can be summarized as follows:

• To develop complementary regularization applied to optical flow problems [25, 26] and proposed by the authors for other applications (challenging tasks specifically for matrix-valued images).

• The application of the direct method of calculus of variation (energy minimization) along with standard finite difference discretization (numerical algorithm) has been applied to optimize the proposed objective function.

• To evaluate the performance of our method, we conducted numerous numerical experiments and compared the results with those of competitive methods. The performance evaluation based on some confidence measures is MSE, PSNR, and SSIM. The rest of this paper is as follows. In Section 2, we briefly review some related work on variational methods for image denoising. In Section 3, we present the formulation of the proposed model and the problem settings. In Section 4, we present problem discretization and image quality assessment. In Section 5, we represent the numerical experiments and simulations with a comparative study. Section 6 is the conclusion of the paper.

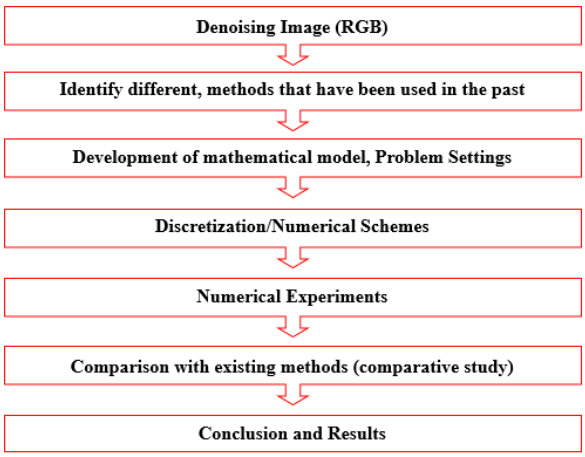

Fig. 1 Flowchart of the research methodology

2. Literature Review

Mathematically, the color noisy image is defined as follows:

$$f: \Omega \subset R^2 \rightarrow R^3 \quad (1)$$

where

$$f = u + \eta \quad (2)$$

Here, the original image is u and noise η, respectively. Image-denoising problems are usually ill-posed and totally data-dependent. Energy minimization techniques are modern regularization methods used to handle mathematical imaging problems [13–17, 25, 26]. The variational methods for image denoising usually minimize the energy functional given below:

$$\min_{u \in \Omega} \left\{ E(u) := \int_{\Omega} M(u, f) \partial\Omega + \int_{\Omega} V(\nabla u) \partial\Omega \right\} \quad (3)$$

A specific example in [38] considered the following energy optimization denoising problem: $E(u)$

$$\min_{u \in \Omega} \left\{ E(u) := \frac{\lambda}{2} \int_{\Omega} (u - f)^2 \partial\Omega + \int_{\Omega} R(u) \partial\Omega \right\} \quad (4)$$

where the domain of the image is Ω with Lipschitz boundary, and $\lambda > 0$.

In mathematical images, denoising problems, total variation, and Tikhonov regularization are well-known nonlinear and linear variational regularization techniques [13, 22]. Considering the extra regularization effects of linear diffusion filters, nonlinear smoothing terms have been preferred for preserving image hypersurfaces during the processing task. Furthermore, the diffusion process has two classes: isotropic and anisotropic diffusion. [39] discusses these diffusion classes in detail. The first part of Eq. (3) measures the fidelity to the data f that minimizes the oscillations in the noisy image called the data term. The second part is the regularization term that performs the smoothing effects called the regularization term. An example of quadratic regularization is the Tikhonov method used as the earliest regularization technique, in which the smoothing part consists of a L^2 (Ω) norm of gradient [22, 40]. Eq. (5) below considers the Tikhonov optimization model:

$$\min_{u \in \Omega} \left\{ E(u) := \int_{\Omega} M(u, f) \partial\Omega + \lambda \int_{\Omega} |\nabla u|^2 \partial\Omega \right\} \quad (5)$$

Famous examples of nonlinear optimization are the optimization of non-quadratic functionals like $L^1(\Omega)$ [13] and the Perona–Malik approach [19]. $L^1(\Omega)$ or total variation regularization preserves the edge information in the recovered image [41]. Total variation regularization is a well-known regularization among edge-preserving regularization methods [13]. [13 and 38] proposed optimization of the $L^1(\Omega)$ norm of the gradient of the image, instead of the $L^2(\Omega)$ norm. The ROF variational model is as follows:

$$\min_{u \in \Omega} \left\{ E(u) := \int_{\Omega} M(u, f) \partial\Omega + \frac{\lambda}{2} \int_{\Omega} |\nabla u| \partial\Omega \right\} \quad (6)$$

The norm $\int_{\Omega} |\nabla| \partial\Omega| \, \partial\Omega$ is the regularization term, and the norm $\int_{\Omega} M(u, f) \partial\Omega$ is the fidelity term. The regularization term measures the amount of oscillation found in the function $u(x, y)$ and allows for discontinuities while disfavoring oscillations. As a result, the TV model performs very well in preserving edges in the recovered image. The ROF model is generally effective in removing Gaussian noise from images. It preserves edges well. However, ROF is observed as losing some geometrical features of the image and causing artifacts such as staircase artifacts [42]. Another very popular and effective approach in the available imaging literature is the Perona–Malik (PM) imaging method, which is an ill-posed and usually called anisotropic diffusion method [19]. They proposed their

Model, which is a classic edge-preserving diffusion model, was used for image processing. The smoothing part of the proposed energy functional is given by

$$V(\nabla u) = \int_{\Omega} \frac{c^2}{2} \log \left(1 + \left(\frac{|\nabla u|}{c} \right)^2 \right) \partial\Omega \quad (7)$$

where c represents a tuning constant.

The choice of data term depends on the imaging application. Visible artifacts have been revealed in the images recovered by the application of the Perona–Malik in homogeneous regions from the energy functional, which lacks the mathematical properties of $|\nabla u|$ for particular values.

3. Proposed Method and Problem Settings

Conventional denoising methods based on variational approaches, as reported in the literature, are usually based on gray value image processing, which is a simple computational task. Considering the availability of modern computers with extended memory and computational power, it would be more interesting to tackle complex computational tasks such as the processing of color imaging. In this work, we propose a minimization problem with a modification in nonlinear regularization based on the [28] energy

functional approach using the idea of complementary data regularization. The complementary regularization proposed for optic flow problems goes back to [25], which introduced the normalization of the data term to maintain a good balance between smoothness and data to avoid the issue of contradiction (which may occur between those terms). Furthermore, the authors assumed the idea of such data normalization (proposed as complementary optic flow) for other imaging tasks, such as image denoising. In the spirit of the above discussion, we propose the following denoising variational model for matrix-valued images as the color image denoising problem.

$$\min_{u\in\Omega}\Big\{E(u_k) \coloneqq \alpha\int_{\Omega} g_k(|\nabla uk|)\partial\Omega + \lambda\int_{\Omega} C_r(|\nabla f_k|)M(u_k,f_k)\partial\Omega\Big\} \tag{8}$$

Here $\alpha > 0$ strictly positive scaling parameter, the diffusivity coefficient $g_k(|\nabla u_k|) \in L^1(\Omega)$ is given as

$$g_k(|\nabla u_k|) = c\left(\sqrt{1+\left(\frac{|\nabla \mathrm{u_k}|}{c}\right)^2}-1\right) \tag{9}$$

$$C_r(|\nabla f_k|) = \frac{1}{1+\frac{|\nabla f_k|^2}{c^2}} \tag{10}$$

$$M(u,f) = (u_k - f_k)^2 \tag{11}$$

The tuning parameter $\lambda > 0$, the small shape defining constant c and $C_r(|\nabla f_k|)$ is the complimentary regularization function, $k = 1,2,3$ represents the respective color channels (R,G,B) of matrix-valued image. For the optima of the energy functional Eq. (8), with the application of the direct method of calculus of variation [43], the optima variational optimization problem given in Eq. (8) yields the Euler-Lagrange equation:

$$-div\left(\alpha g_k^{'}(|\nabla u_k(x,y)|)\nabla u_k(x,y)\right) + \lambda C_r(|\nabla u_k(x,y)|)(u_k - f_k) = 0 \tag{12}$$

with the Neumann boundary condition

$$\frac{\partial u_k(x,y)}{\partial n} = 0, \quad \partial\Omega$$

where

$$g_k^{'}\left(\left|\nabla u_{k(x,y)}\right|\right) = \frac{1}{\sqrt{1+\frac{|\nabla u_k|^2}{c^2}}}$$

The solution of problem (12) is therefore equivalently viewed as the steady-state solution to the time-dependent problem given in Eq. (13)

$$u_t(x,y,t) = div(\alpha g_k^{'}(|\nabla u_k(x,y,z)|)\,\nabla u_k(x,y,t)) - \lambda C_r(|\nabla f_k(x,y,z)|)(u_k - f_k) \tag{13}$$

with boundary conditions

$$\frac{\partial u_k(x,y,t)}{\partial n} = 0, \text{ on } \partial\Omega\times(0,T)$$

and the initial conditions

$$u_k(x,y,0) = f_k(x,y) \text{ in } \Omega$$

where

$$g_k^{'}\left(\left|\nabla u_{k(x,y,t)}\right|\right) = \frac{1}{\sqrt{1+\frac{|\nabla u_k|^2}{c^2}}}$$

4. Problem Discretization

To design the solution strategy and the locally adaptive regularization algorithm, we apply the standard finite differences to discretize the continuous problem (13). Furthermore, we introduce the following gradient approximation for the image gradients ∇u_k.

$$\nabla_N u_k(i,j,t) \approx \frac{u_k(i-1,j)-u_k(i,j)}{\Delta x} \tag{14}$$

$$\nabla_S u_k(i,j,t) \approx \frac{u_k(i+1,j)-u_k(i,j)}{\Delta x} \tag{15}$$

$$\nabla_E u_k(i,j,t) \approx \frac{u_k(i,j+1)-u_k(i,j)}{\Delta y} \tag{16}$$

$$\nabla_W u_k(i,j,t) \approx \frac{u_k(i,j-1)-u_k(i,j)}{\Delta y} \tag{17}$$

where $\nabla_N u_k(i,j,t)$,$\nabla_s u_k(i,j,t)$, $\nabla_E u_k(i,j,t)$ and $\nabla_W u_k(i,j,t)$ are the components of (18) in the north, south, east and west, respectively, at time t.

Furthermore, we consider the space discretization steps as $\Delta x = \Delta y = 1$. The time step is denoted as Δt. Substituting the above finite differences in (13), and by simplification, the final discrete problem is given as follows:

$$\begin{aligned} u_k(i,j,t+1) = u_k &+ \Delta t[\alpha(g_N\nabla_N u_k + g_S\nabla_S \mathrm{u_k} \\ &+ g_E\nabla_E u_k + g_w\nabla_w u_k) \\ &- \lambda(c_N(u_k - f_k)c_S(u_k - f_k) \\ &+ c_E(u_k - f_k) \\ &+ c_W(u_k - f_k))] \end{aligned} \tag{18}$$

where the diffusivity functions are computed as:

$$g_p = g\left(\left|\nabla_p u_k(i,j)\right|\right) = \frac{1}{\sqrt{1+\frac{|\nabla u_k|^2}{c^2}}} \tag{19}$$

$$c_p = C_r\left(\left|\nabla_p f_k(i,j)\right|\right) = \frac{1}{1+\frac{|\nabla f_k|^2}{c^2}} \tag{20}$$

where $p = (N,S,E,W)$.

It is generally observed that explicit numerical schemes are usually conditionally stable; therefore, extra care is required to keep the central coefficient positive for the stencil of the derived numerical scheme. In this case, bounding diffusion time controls the stability requirement. We consider the time step as $0 \le \Delta t \le 0.25$ that fulfills the Friedrichs Lewy (CFL) stability condition [44]. All experiments of the derived numerical scheme used Matlab R2018a for Windows 10 on a PC with Intel(R) Core(TM) i7-5500U CPU @ 2.40GHz 2.40 GHz Intel (R) Core(TM) 2 Duo CPU and 8.00 GB of RAM. The computational algorithm is demonstrated as a flow chart in Fig. 1.

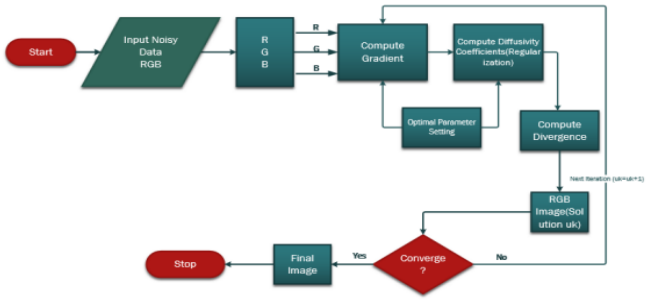

Fig. 2 Proposed algorithm (Developed by the authors)

4.1. Image Quality Assessment Indicators

To demonstrate the performance of the proposed method, some image quality assessment indicators have been considered. It has been observed in the literature that the appropriate quality assessment parameters for quantitative and visual quality assessment are peak signal-to-noise ratio (PSNR) and structural similarity index measurements (SSIM) [30, 45]. The higher the PSNR value, the better the image recovery. Mathematically, the signal-to-noise ratio is defined as

$$PSNR = 20\log_{10}\left(\frac{MAX_{uk}}{\sqrt{MSE_k}}\right) \quad (21)$$

$$MSE_k = \frac{1}{3}\left(mse_r + mse_g + mse_b\right) \quad (22)$$

$$mse_k = \sum_{i=1}^{m}\sum_{j=1}^{n}\left(g_k(i,j) - u_k(i,j)\right)^2 \quad (23)$$

The numbers m, n denote the width and length of the image. MAX_{uk} denotes the largest value of the pixel in the image. The evaluation based on structural similarity index measurements (SSIM) is correlated to the human visual system (HVS). Furthermore, the bounds for SSIM values are given here as SSIM $\in [0, 1]$, the values of SSIM closer to 1, yield the better structure retention of the image.

$$SSIM = \frac{\left(2\mu_{uk}\mu_{fk} + c_1\right)\left(2\sigma_{ukfk} + c_2\right)}{\left(\mu_{uk}^2 + \mu_{fk}^2 + c_1\right)\left(\sigma_{uk}^2 + \sigma_{fk}^2 + c_2\right)} \quad (24)$$

where u_k is the recovered image and μ denotes the mean, σ denotes the covariance, c_1 and c_2 denotes the constants.

5. Numerical Experiments and Simulation

In this section, we apply the proposed computational algorithm and numerical scheme to noisy matrix-valued (color) images. To demonstrate the performance of the proposed method, we conducted three types of experiments on color images: Baboon, Barbara, and House as benchmark datasets (images). The datasets are from the USC-SIPI Image Database (http://sipi.usc.edu/database/) (see Fig. 3). For different experiments and a fair comparison with classical methods, Gaussian noise with various values of standard deviation σ has been added to the original images, whereas the selection of other regularization parameters is discussed as follows.

5.1. Selection of Appropriate Parameters

Considering the inverse nature of the denoising problems, the regularization parameters play an important role, specifically in variational models. The variational models are composed of regularization and data parts, but the level of contribution from both parts remains a question: which part contributes to the role of main smoothness? Therefore, these scaling parameters usually function as controlling agents in estimating the smooth solution to the ill-posed problem. Such tuning parameters improve the quality of image diffusion during the denoising process. There are two ways for the appropriate selection of the regularization, either manually [19, 22, 46] or in a locally adaptive way [26, 47, 48]. Regularization in a locally adaptive way is also interesting and improves the smoothness at each adaptive step of the regularization of the solution [26, 47, and 48]. In this study, we establish a computational strategy using manual adaptation with an appropriate choice of tuning parameters by keeping uniform over the entire domain. Such a choice will allow us to develop local and automatic adaptive procedures for matrix-valued imaging methods.

(a) Barbara (b) House (c) Baboon

Fig. 3 Original images (http://sipi.usc.edu/database/)

We start our experiments with Barbara, image of size 512 × 512, Fig. 3a, by adding Gaussian noise with mean μ = 0. Furthermore, we conducted experiments on the images at different noise levels of the standard deviation $\sigma = 30$ and $\sigma = 50$, as shown in Figs. 4a and 4b. In the derived discrete scheme

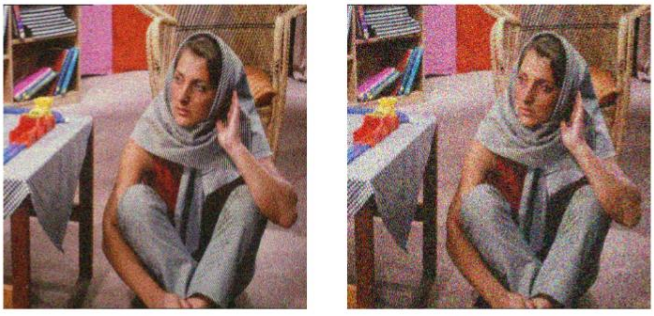

(a) $\sigma = 30$ (b) $\sigma = 50$

Fig. 4 Noisy image Barbara (Developed by the authors)

The parameters like λ and c have been fixed as λ = 0.05 and c = 15, and the experiments have been conducted for various choices of the regularization

parameter α. Furthermore, the simulation results show that the variations in the smoothing parameter α reveal significant regularization effects on the recovered images. From the overall performance of our algorithm, the proposed method works well and successfully removes noise along with sharper edge recovery. Figs. 5 and 6 and Table 1 present the numerical results and show that the choice of the parameter up to α = 10 yields good quality results, and the proposed method effectively removes noise and protects meaningful image features. Furthermore, with the increase in the value of scaling parameter α, the diffusion becomes fast; therefore, extra blurring effects appear in the image, and consequently, the quality reduces.

(a) $\alpha = 6$ (b) $\alpha = 10$ (c) $\alpha = 15$ (d) $\alpha = 20$ (e) $\alpha = 50$

Fig. 5 Image recovery of the Barbara image with different values of smoothing parameter α and noise level $\sigma = 30$ (Developed by the authors)

(a) $\alpha = 6$ (b) $\alpha = 10$ (c) $\alpha = 15$ (d) $\alpha = 20$ (e) $\alpha = 50$

Fig. 6 Results for noise level $\sigma = 50$ (Developed by the authors)

For the study of the quality variation in the solution images, the reader can see the results of quality assessment parameters such as SSIM and PSNR (Table 1).

Table 1 Computational time, PSNR, and SSIM of Barbara image (Developed by the authors)

Method	α	PSNR	SSIM	Time(s)	Iteration(s)
	$\sigma = 30$				
Proposed	6	26.7061	0.8366	3.3709	23
	10	26.5836	0.8304	5.4367	14
	20	26.0732	0.8136	3.9345	07
	30	25.3137	0.7988	1.5518	05
	50	23.8945	0.7668	0.6582	03
	$\sigma = 50$				
Proposed	6	25.0279	0.7729	8.5548	46
	10	24.8591	0.7586	5.7188	26
	20	24.3144	0.7310	4.0521	13
	30	23.6367	0.7078	1.8715	8
	50	22.1381	0.6750	0.8378	5

The second experiment considers the image house of size 512 × 512 (Fig. 3b) degraded by adding Gaussian noise of density $\sigma = 30$ and $\sigma = 50$, see Figs. 7a and 7b. We applied quantitative and visual quality measures to examine the performance of the proposed method. The qualitative and quantitative performance of the proposed method for this image is also good, as shown in Figs. 8a–8h; Table 2 presents the quality measures.

(a) $\sigma = 30$ (b) $\sigma = 50$

Fig. 7 Noisy image house (Developed by the authors)

In this house image, numerous tests are performed. Fig. 8 and Table 2 depict the obtained results.

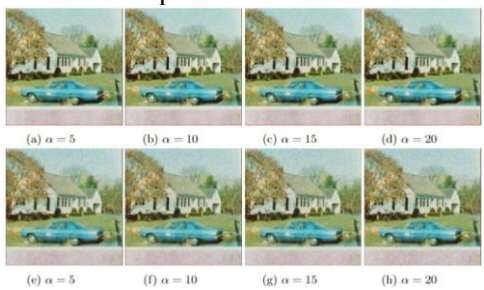

(a) $\alpha = 5$ (b) $\alpha = 10$ (c) $\alpha = 15$ (d) $\alpha = 20$

(e) $\alpha = 5$ (f) $\alpha = 10$ (g) $\alpha = 15$ (h) $\alpha = 20$

Fig. 8 Evaluation of proposed method on noisy house image, variance $\sigma = 30$ and $\sigma = 50$ at different values of α (Developed by the authors)

The results show that the proposed method performs well with respect to the increase in the noise level. In this experiment, we present a line plot for a clear understanding of the results, see Fig. 9.

Table 2 Computational time, PSNR, and SSIM of the house image (Developed by the authors)

Method	α	PSNR	SSIM	Time(s)	Iteration(s)
	$\sigma = 30$				
Proposed	5	27.1767	0.8473	7.5119	27
	10	27.0336	0.8374	3.2808	13
	20	26.5078	0.8216	2.1657	09
	30	25.7085	0.8056	1.8352	07
	$\sigma = 50$				
Proposed	5	24.9911	0.7728	14.952	53
	10	24.8014	0.7573	5.8112	24
	20	24.3219	0.7301	3.6996	15
	30	23.7034	0.7100	2.7455	11

In the third series of experiments, the Baboon image of the size 512 × 512 is considered, see Fig. 3c. The random noise with zero mean and varying values of the standard deviation levels as $\sigma = 15, \sigma = 30$ and $\sigma = 50$ is added (see the degraded images in Figs. 10a, 10b, 10c).

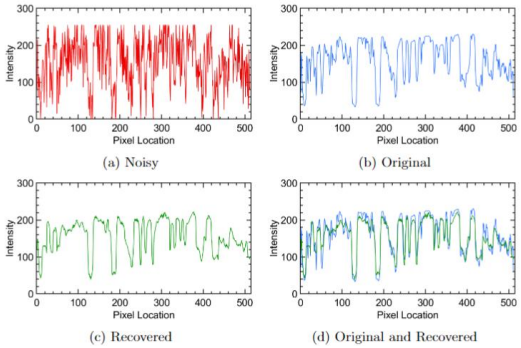

(a) Noisy (b) Original

(c) Recovered (d) Original and Recovered

Fig. 9 Line graph of the house image (Developed by the authors)

The proposed method is employed for the distorted image (noisy), as shown in Fig. 10. The visual results demonstrate that our method works effectively for image recovery, which is a challenging task specifically for baboon-like complicated images with sharp edges. Table 3 and Figs. 11a-11o show the simulation results and computational time.

Table 3 Computational time, PSNR, and SSIM of baboon image (Developed by the authors)

Method	α	PSNR	SSIM	Time(s)	Iteration(s)
	$\sigma = 15$				
Proposed	06	26.7686	0.9276	3.2491	16
	10	26.7069	0.9268	3.9208	13
	20	20.4356	0.9237	5.3900	22
	30	20.3343	0.9208	2.8684	12
	50	19.7580	0.9038	1.5278	6
	$\sigma = 30$				
Proposed	06	23.0460	0.8228	3.6015	15
	10	23.0390	0.8230	2.5404	09
	20	22.9460	0.8203	1.2441	05
	30	22.6939	0.8172	0.9779	04
	50	21.8539	0.8042	0.7335	03
	$\sigma = 50$				
Proposed	06	20.9871	0.6983	7.3350	31
	10	21.0104	0.7008	4.3314	04
	20	20.9115	0.6995	2.1904	09
	30	20.7071	0.6947	1.4551	06
	50	20.9849	0.6852	0.9715	04

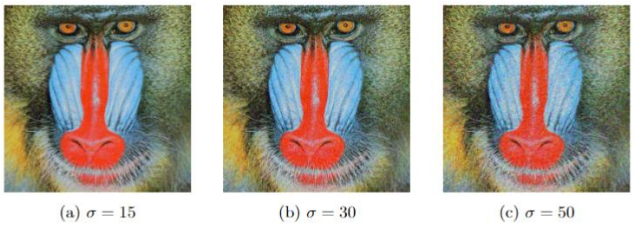

Fig. 10 Noisy image of baboon (Developed by the authors)

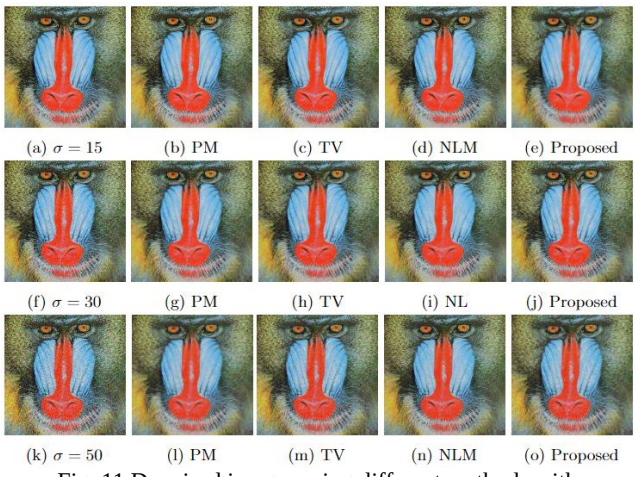

Fig. 11 Denoised images using different methods with variance $\sigma = 15$,$\sigma = 30$ and $\sigma = 50$ (Developed by the authors)

5.2. Comparison of Results

Finally, the performance of the proposed method is validated with a comparative study with well-existing methods such as the Prona–Malik (PM) method [19], total variation (TV) regularization [22], and non-local mean (NLM) [46]. Such methods usually adopt the manual method of the choice for tuning parameters. In these methods, these parameters were selected uniformly on the whole domain as k = 15, λ = 0.05, and ε = 0.0000001, respectively. The results of the NLM method were obtained using an online free available simulator available at https: //doi.org/10.5201/ipol.2011.bcmnlm. The results for other methods, such as TV and Perona-Malik models, have been computed for color images in the same settings as those given in the proposed algorithm. The proposed method takes less computational time, which is a good aspect compared to the existing robust methods [19, 22, and 46] with better visual quality results presented in Tables 4 and 5 and depicted in Figs. 11d, 11i, and 11m. The PM model generates undesirable artifacts with less visual quality 11b, 11g, and 11l than the proposed method. The total variation regularization method yields better values for the noise levels of standard levels σ = 15 and σ = 30 but generates, resulting in more contrast degradation and takes more computational time as compared to the proposed method. For details, the reader can see Tables 4 and 5 and Figs. 11c, 11h, and 11m.

Table 4 Comparative study with classical methods (Developed by the authors)

Images	$\sigma = 30$				
	Methods	PSNR	SSIM	Time(s)	Iteration(s)
Barbara	PM	26.4523	0.8359	5.30611	31
	TV	26.6786	0.8361	51.2595	299
	NLM	19.3445	-	-	-
	Proposed	26.7061	0.8366	3.3709	23
House	PM	26.8021	0.8349	5.4419	30
	TV	26.8550	0.8370	55.7100	289
	NLM	19.4040	-	-	-
	Proposed	27.0336	0.8374	3.2808	13
Baboon	PM	22.7742	0.8211	3.8711	08
	TV	23.0233	0.8209	6.0410	22
	NLM	20.5041	-	-	-
	Proposed	23.0390	0.8230	2.5404	09

Table 5 Comparative study with classical methods (Developed by the authors)

Images	$\sigma = 50$				
	Methods	PSNR	SSIM	Time(s)	Iteration(s)
Barbara	PM	24.4002	0.7551	10.5908	80
	TV	22.5126	0.6405	50.7645	327
	NLM	19.6565	-	-	-
	Proposed	24.8591	0.7586	5.7188	26
House	PM	24.1629	0.7557	13.6550	74
	TV	22.7098	0.6545	66.6322	327
	NLM	19.6464	-	-	-
	Proposed	24.8014	0.7583	5.8112	24
Baboon	PM	20.6666	0.6936	10.5906	61
	TV	20.6565	0.6999	58.4949	327
	NLM	19.6060	-	-	-
	Proposed	21.0104	0.7008	4.3314	4

6. Conclusion

In this study, the results from the matrix-valued

image noise removal nonlinear method with the data normalization approach are analyzed and presented. Experimental results reveal that our proposed method reduces computational time and generates promising image results compared with classical methods such as Perona–Malik and TV methods. Comparing the proposed method with the classical methods, the proposed method significantly reduces noise. The comparative analysis emphasizes the potential benefits of nonlinear isotropic diffusion techniques and the potential for regularizing data to maintain the balance between regularization and data terms for noise removal in distorted images. It has been observed from the observed results, such as SSIM, PSNR, and computational time, that the proposed modified model can simultaneously remove noise, preserve edges, and suppress staircases. From the overall performance of the proposed method, the modified model yields good results in quality analysis for color images and reveals the significant effects of regularization from complementary data regularization and the contribution of appropriate tuning parameters. It is observed from the computed results from this proposed method that a reasonable possibility of improvement in available classical methods is still available. Further improvements are possible for these methods to make them more useful in theoretical and practical settings. As in this work, the tuning parameters have been selected uniformly on the whole computation domain, but it is also possible to select locally in an adaptive way. Such a locally adaptive way for selecting smoothing parameters is also an attractive aspect to apply to the diffusion part of the energy, which is under consideration for our upcoming paper..

References

[1] FU B., ZHAO X., SONG C., LI X., and WANG X. A salt and pepper noise image denoising method based on the generative classification. *Multimedia Tools and Applications*, 2019, 78: 12043-12053. https://doi.org/10.1007/s11042-018-6732-8

[2] LUISIER F., BLU T., and UNSER M. Image denoising in mixed Poisson–Gaussian noise. *IEEE Transactions on image processing*, 2010, 20(3): 696-708. https://doi.org/10.1007/s10851-021-01033-310.1109/TIP.2010.2073477

[3] JIN Q., GRAMA I., and LIU Q. Poisson Shot Noise Removal by an Oracular Non-Local Algorithm. *Journal of Mathematical Imaging and Vision*, 2021, 63: 855-874. https://doi.org/10.1007/s10851-021-01033-3

[4] BOYAT A., and JOSHI B.K. November. Image denoising using wavelet transform and median filtering. In: *2013 Nirma University International Conference on Engineering (NUiCONE)*, 2013: 1-6. https://doi.org/10.1109/NUiCONE.2013.6780128

[5] YU, J. CHEN, L. ZHOU S., WANG L., LI H., and HUANG S. Adaptive image denoising for speckle noise images based on fuzzy logic. *International Journal of Imaging Systems and Technology*, 2020, 30(4): 1132-1142. https://doi.org/10.1002/ima.22442

[6] MOTWANI M.C., GADIYA M.C., MOTWANI R.C., and HARRIS F.C. Survey of image denoising techniques. *Proceedings of GSPX*, 2004, 27: 27-30. https://api.semanticscholar.org/CorpusID:17594958.

[7] JAIN P., and TYAGI V. A survey of edge-preserving image denoising methods. *Information Systems Frontiers*, 2016, 18: 159-170. https://doi.org/10.1007/s10796-014-9527-0

[8] DOUGHERTY G. *Medical image processing: Techniques and applications*. Springer, 2011. https://doi.org/10.1007/978-1-4419-9779-1

[9] BOYAT A.K., and JOSHI B.K. A review paper: noise models in digital image processing. *Signal & Image Processing*, 2015, 6(2). https://doi.org/10.48550/arXiv.1505.03489

[10] WEN Y.-W., CHING W.-K., and NG M. A semi-smooth newton method for inverse problem with uniform noise. *Journal of Scientific Computing*, 2018, 75(2): 713-732. https://doi.org/10.1007/s10915-017-0557-x

[11] KAMALAVENI V., RAJALAKSHMI R.A., and NARAYANANKUTTY K.A. Image denoising using variations of Perona-Malik model with different edge stopping functions. *Procedia Computer Science*, 2015, 58: 673-682. https://doi.org/10.1016/j.procs.2015.08.087

[12] ZHANG W., CAO Y., ZHANG R., and WANG Y. Image denoising using total variation model guided by steerable filter. *Mathematical Problems in Engineering*, 2014, Article ID 423761. https://doi.org/10.1155/2014/423761

[13] RUDIN L.I., OSHER S., and FATEMI E. Nonlinear total variation based noise removal algorithms, *Physica D: Nonlinear Phenomena*, 1992, 60(1-4). https://doi.org/10.1016/0167-2789 (92)90242-F

[14] LIU X., and HUANG L. A new nonlocal total variation regularization algorithm for image denoising. *Mathematics and Computers in Simulation*, 2014, 97: 224-233. https://doi.org/10.1016/j.matcom.2013.10.001

[15] OH S., WOO H., YUN S., and KANG M. Non-convex hybrid total variation for image denoising. *Journal of Visual Communication and Image Representation*, 2013, 24(3): 332-344. https://doi.org/10.1016/j.jvcir.2013.01.010

[16] MA G., YAN Z., LI Z., and ZHAO Z. Efficient iterative regularization method for total variation-based image restoration. *Electronics*, 2022, 11(2): 258. https://doi.org/10.3390/electronics11020258

[17] LIU K., TAN J., and SU B. An adaptive image denoising model based on Tikhonov and TV regularizations. *Advances in Multimedia*, 2014, Article ID 934834. https://doi.org/10.1155/2014/934834

[18] AMUR K.B. Some regularization strategies for an ill-posed denoising problem, *International Journal of Tomography and Statistics*, 2012, 19(1): 46-59. http://www.ceser.in/ceserp/index.php/ijts/article/view/232

[19] PERONA P., and MALIK J. Scale-space and edge detection using anisotropic diffusion. *IEEE Transactions on Pattern Analysis and Machine Intelligence*, 1990, 12(7): 629-639. https://doi.org/10.1109/34.56205

[20] YUAN J., and WANG J. Perona-malik model with a new diffusion coefficient for image denoising. *International Journal of Image and Graphics*, 2016, 16(02), 1650011. https://doi.org/10.1142/S021946781650011X

[21] WIELGUS M. *Perona-Malik equation and its*

numerical properties. Bachelor thesis of 2010, Faculty of Mathematics, Informatics and Mechanics, University of Warsaw. 2014. https://doi.org/10.48550/arXiv.1412.6291
[22] TIKHONOV A.N., and ARSENIN V.I.A.K. *Solutions of ill-posed problems*. Winston, 1977. https://doi.org/10.2307/2006360
[23] NCHAMA G.A.M., MECIAS A.L., and RICARD M.R. Perona-Malik model with diffusion coefficient depending on fractional gradient via Caputo-Fabrizio derivative. *Abstract and Applied Analysis*, 2020, Article ID 7624829. https://doi.org/10.1155/2020/7624829
[24] DUAN J. *Variational and PDE-based methods for image processing*. Doctoral dissertation, University of Nottingham, 2018.
[25] ZIMMER H., BRUHN A., WEICKERT J., VALGAERTS L., SALGADO A., ROSENHAHN B., and SEIDEL H.-P. Complementary Optic Flow. In: *International Workshop on Energy Minimization Methods in Computer Vision and Pattern Recognition.* 2009: 207-220. https://doi.org/10.1007/978-3-642-03641-5_16
[26] AMUR K.B. A posteriori control of regularization for complementary image motion problem. *Sindh University Research Journal* (Science Series), 2013, 45(3). https://sujo.usindh.edu.pk/index.php/SURJ/issue/archiv
[27] MAISELI B. Nonlinear anisotropic diffusion methods for image denoising problems: Challenges and future research opportunities. *Array*, 2023, 17, 100265. https://doi.org/10.1016/j.array.2022.100265
[28] CHARBONNIER P., BLANC-FERAUD L., AUBERT G., and BARLAUD M. Deterministic edge-preserving regularization in computed imaging. *IEEE Transactions on Image Processing*, 1997, 6(2): 298-311. https://doi.org/10.1109/83.551699
[29] ALLY N., NOMBO J., IBWE K., ABDALLA A.T., and MAISELI B.J. Diffusion-driven image denoising model with texture preservation capabilities. *Journal of Signal Processing Systems*, 2021, 93: 937-949. https://doi.org/10.1007/s11265-020-01621-3
[30] WANG Z., BOVIK A.C., SHEIKH, H.R., and SIMONCELLI E.P. Image quality assessment: from error visibility to structural similarity. *IEEE Transactions on Image Processing*, 2004, 13(4): 600-612. https://doi.org/10.1109/TIP.2003.819861
[31] WANG Y., REN W., and WANG H. Anisotropic second and fourth order diffusion models based on convolutional virtual electric field for image denoising. *Computers & Mathematics with Applications*, 2013, 66(10): 1729-1742. https://doi.org/10.1016/j.camwa.2013.08.034
[32] CHANG S.G., YU B., and VETTERLI M. Adaptive wavelet thresholding for image denoising and compression. *IEEE Transactions on Image Processing*, 2000, 9(9): 1532-1546. https://doi.org/10.1109/83.862633
[33] YAN R., SHAO L., LIU L., and LIU Y. Natural image denoising using evolved local adaptive filters. *Signal Processing*, 2014, 103: 36-44. https://doi.org/10.1016/j.sigpro.2013.11.019
[34] HU J., and LUO Y.P. Non-local means algorithm with adaptive patch size and bandwidth. *Optik*, 2013, 124(22): 5639-5645. https://doi.org/10.1016/j.ijleo.2013.04.009
[35] DABOV K., FOI A., KATKOVNIK V., and EGIAZARIAN K. Color image denoising via sparse 3D collaborative filtering with grouping constraint in luminance-chrominance space. In: *2007 IEEE international conference on image processing*, 2007, 1: 313-316. https://doi.org/10.1109/ICIP.2007.4378954
[36] JIA H., YIN Q., and LU M. Blind-noise image denoising with block-matching domain transformation filtering and improved guided filtering. *Scientific Reports*, 2022, 12(1), 16195. https://doi.org/10.1038/s41598-022-20578-w
[37] PIRZADA M., AMUR K.B., ARAIN M.B., and MALOOKANI R.A. Image Driven Isotropic Diffusivity and Complementary Regularization Approach for Image Denoising Problem. *VFAST Transactions on Mathematics*, 2022, 10: 1-13. https://doi.org/10.21015/vtm.v10i1.1186
[38] RUDIN L.I., OSHER S., and FATEMI E. Nonlinear total variation based noise removal algorithms. *Physica D: Nonlinear Phenomena*, 1992, 60(1-4): 259-268. https://doi.org/10.1016/0167-2789(92)90242-F
[39] WEICKERT J. *Anisotropic diffusion in image processing*. Vol. 1. Teubner, Stuttgart, 1998. http://www.lpi.tel.uva.es/muitic/pim/docus/anisotropic_diffusion.pdf
[40] PÖSCHL C. *Tikhonov regularization with general residual term*. Ph.D. thesis. Alpine-Adriatic University, 2008.
[41] ESEDOGLU S., and OSHER S.J. Decomposition of images by the anisotropic Rudin- Osher- Fatemi model. *Communications on Pure and Applied Mathematics*, 2004, 57(12): 1609-1626. https://doi.org/10.1002/cpa.20045
[42] PAPAFITSOROS K., and SCHÖNLIEB C.B. A combined first and second order variational approach for image reconstruction. *Journal of mathematical imaging and vision*, 2014, 48: 308-338. https://doi.org/10.1007/s10851-013-0445-4
[43] GELFAND I.M., and SILVERMAN R.A. *Calculus of variations*. Courier Corporation, 2000. https://thuvienso.hoasen.edu.vn/bitstream/handle/123456789/8961/Contents.pdf?sequence=3
[44] HÖLLIG K. Existence of infinitely many solutions for a forward backward heat equation. *Transactions of the American Mathematical Society*, 1983, 278(1): 299-316. https://www.ams.org/tran/1983-278-01/S0002-9947-1983-0697076-8/S0002-9947-1983-0697076-8.pdf
[45] WANG Z., and BOVIK A.C. Mean squared error: Love it or leave it? A new look at signal fidelity measures. IEEE Signal Processing Magazine, 2009, 26(1): 98-117. https://doi.org/10.1109/MSP.2008.930649
[46] BUADES A., COLL B., and MOREL J.M. A non-local algorithm for image denoising. In: *2005 IEEE Computer Society Conference on Computer Vision and Pattern Recognition (CVPR'05), San Diego, CA, USA*. 2005, 2: 60-65. https://doi.org/10.1109/CVPR.2005.38
[47] GRASMAIR M. Locally Adaptive Total Variation Regularization, In: *Scale Space and Variational Methods in Computer Vision, Second International Conference, 2009, Voss, Norway, 2009, June 1-5*. 2009. http://dx.doi.org/10.1007/978-3-642-02256-2_28
[48] AMUR K.B., MEMON A.L., and QURESHI S. FEM based approximations for the TV denoising optimization problem. *Mehran University Research Journal of Engineering & Technology*, 2014, 33(1): 121-128. http://publications.muet.edu.pk/research_papers/pdf/pdf848.pdf

参考文:

[1] FU B., ZHAO X., SONG C., LI X. 和 WANG X. 一種基於生成分類的椒鹽噪聲圖像去噪方法。多媒體工具與應用，2019，78：12043-12053。https://doi.org/10.1007/s11042-018-6732-8

[2] LUISIER F.、BLU T. 和 UNSER M。混合泊松-高斯雜訊中的影像去雜訊。IEEE影像處理彙刊，2010，20(3)：696-708。https://doi.org/10.1007/s10851-021-01033-310.1109/TIP.2010.2073477

[3] JIN Q., GRAMA I. 和 LIU Q. 透過神論非局部演算法去除泊鬆散粒噪聲。數學成像與視覺雜誌，2021，63：855-874。https://doi.org/10.1007/s10851-021-01033-3

[4] BOYAT A.和 JOSHI B.K. 十一月。使用小波變換和中**值**濾波進行影像去雜訊。請參**閱**：2013年尼爾瑪大學國際工程會議，2013：1-6。https://doi.org/10.1109/NUiCONE.2013.6780128

[5] YU, J. CHEN, L. ZHOU S., WANG L., LI H. 和 HUANG S. 基於模糊邏輯的散斑雜訊影像自適應去雜訊。國際影像系統與技術雜誌，2020, 30(4): 1132-1142。https://doi.org/10.1002/ima.22442

[6] MOTWANI M.C., GADIYA M.C., MOTWANI R.C. 和 HARRIS F.C. 影像去雜訊技術綜述。GSPX會議記**錄**，2004年，27：27-30。https://api.semanticscholar.org/CorpusID:17594958。

[7] JAIN P. 和 TYAGI V. 邊**緣**保留影像去噪方法的調**查**。資訊系統前沿，2016，18：159-170。https://doi.org/10.1007/s10796-014-9527-0

[8] DOUGHERTY G. 醫學影像處理：技術與應用。施普林格，2011。https://doi.org/10.1007/978-1-4419-9779-1

[9] BOYAT A.K. 和 JOSHI B.K. 評論論文：數位影像處理中的雜訊模型。訊號與影像處理，2015，6(2)。https://doi.org/10.48550/arXiv.1505.03489

[10] WEN Y.-W., CHING W.-K. 和 NG M. 均**勻**噪音反問題的半光滑牛頓法。科學計算學報， 2018, 75(2): 713-732. https://doi.org/10.1007/s10915-017-0557-x

[11] KAMALAVENI V.、RAJALAKSHMI R.A. 與 NARAYANANKUTTY K.A. 使用具有不同邊**緣**停止函數的佩羅納-馬利克模型變體進行影像去噪。計算機科學，2015，58：673-682。https://doi.org/10.1016/j.procs.2015.08.087

[12] ZHANG W., CAO Y., ZHANG R. 和 WANG Y. 可操縱濾波器引導下的全變分模型影像去雜訊。工程中的數學問題，2014年，文章ID 423761。https://doi.org/10.1155/2014/423761

[13] RUDIN L.I.、OSHER S. 和 FATEMI E. 基於非線性全變分的噪音消除演算法，物理學D：非線性現象，1992，60(1-4)。https://doi.org/10.1016/0167-2789 (92)90242-F

[14] LIU X. 和 HUANG L. 一種新的非局部全變分正則化影像去噪演算法。數學與計算機仿真，2014，97：224-233。https://doi.org/10.1016/j.matcom.2013.10.001

[15] OH S., WOO H., YUN S. 和 KANG M. 影像去噪的非凸混合全變分。視覺傳達與圖像表達學報，2013，24(3)：332-344。https://doi.org/10.1016/j.jvcir.2013.01.010

[16] MA G., YAN Z., LI Z. 和 ZHAO Z. 基於全變分的影像恢復的高效迭代正則化方法。電子學，2022，11（2）：258。https://doi.org/10.3390/electronics11020258

[17] LIU K.，TAN J. 和 SU B. 基於吉洪諾夫和TV正則化的自適應影像去噪模型。多媒體進展，2014年，文章ID 934834。https://doi.org/10.1155/2014/934834

[18] AMUR K.B. 不適定去噪問題的一些正規化策略，國際斷層掃描與統計雜誌，2012，19（1）：46-59。http://www.ceser.in/ceserp/index.php/ijts/article/view/232

[19] PERONA P. 和 MALIK J。使用各向異性擴散進行尺度空間和邊**緣**檢測。電機與電子工程師學會模式分析與機器智能彙刊，1990，12(7)：629-639。https://doi.org/10.1109/34.56205

[20] YUAN J. 和 WANG J. 佩羅納-馬利克模型，具有新的圖像去噪擴散係數。國際圖像與圖形雜誌，2016，16（02），1650011。https://doi.org/10.1142/S021946781650011X

[21] WIELGUS M. 佩羅納-馬利克方程式及其數**值**特性。2010年學士論文，數學、資訊學和力學學院，華沙大學。2014年。https://doi.org/10.48550/arXiv.1412.6291

[22] TIKHONOV A.N. 和 ARSENIN V.I.A.K. 不適定問題的解決方案。**溫**斯頓，1977。https://doi.org/10.2307/2006360

[23] NCHAMA G.A.M.、MECIAS A.L. 和 RICARD M.R.，佩羅納-馬利克模型，其擴散係數取決於 卡普托-法布里奇奧導數的分數梯度。摘要與應用分析，2020年，文章ID 7624829。https://doi.org/10.1155/2020/7624829

[24] DUAN J. 基於變分和偏微分方程的影像處理方法。博士論文，諾丁漢大學，2018。

[25] ZIMMER H.、BRUHN A.、WEICKERT J.、VALGAERTS L.、SALGADO A.、ROSENHAHN B. 和 SEIDEL H.-P。互補光流。請參**閱**：計算機視覺和模式識別中能量最小化方法國際研討會。2009：207-220。https://doi.org/10.1007/978-3-642-03641-5_16

[26] AMUR K.B. 互補影像運動問題正規化的後驗控制。信德大學研究期刊（科學系列），2013，45（3）。https://sujo.usindh.edu.pk/index.php/SURJ/issue/archiv

[27] MAISELI B. 影像去噪問題的非線性各向異性擴散方法：挑戰和未來的研究機會. 大批, 2023, 17, 100265。https://doi.org/10.1016/j.array.2022.100265

[28] CHARBONNIER P.、BLANC-FERAUD

L.、AUBERT G. 和 BARLAUD M. 計算成像中的確定性邊緣保留正則化，電機與電子工程師學會圖像處理彙刊，1997，6(2)：298-311。https://doi.org/10.1109/83.551699
[29] ALLY N.、NOMBO J.、IBWE K.、ABDALLA A.T. 和 MAISELI B.J. 具有紋理保留功能的擴散驅動影像去雜訊模型。訊號處理系統雜誌，2021，93：937-949。https://doi.org/10.1007/s11265-020-01621-3
[30] WANG Z.，BOVIK A.C.，SHEIKH，H.R. 和 SIMONCELLI E.P. 影像品質評估：從錯誤可見性到結構相似性。電機與電子工程師學會影像處理彙刊，2004年，13(4)：600-612。https://doi.org/10.1109/TIP.2003.819861
[31] WANG Y.，REN W. 和 WANG H. 基於卷積虛擬電場的影像去噪各向異性二階和四階擴散模型。計算機與數學及其應用，2013，66(10)：1729-1742。https://doi.org/10.1016/j.camwa.2013.08.034
[32] CHANG S.G.，YU B.，和 VETTERLI M. 用於影像去雜訊和壓縮的自適應小波閾值。電機與電子工程師學會 影像處理彙刊，2000 年，9(9)：1532-1546。https://doi.org/10.1109/83.862633
[33] YAN R.，SHAO L.，LIU L. 和 LIU Y.使用進化局部自適應濾波器的自然影像去噪。訊號處理，2014，103：36-44。https://doi.org/10.1016/j.sigpro.2013.11.019
[34] HU J. 和 LUO Y.P. 具有自適應補丁大小和頻寬的非局部均值演算法。光學，2013, 124(22): 5639-5645。https://doi.org/10.1016/j.ijleo.2013.04.009
[35] DABOV K.、FOI A.、KATKOVNIK V. 和 EGIAZARIAN K. 透過在亮度-色度空間中具有分組約束的稀疏3D協同過濾進行彩色影像去噪。請參閱：2007年電機與電子工程師學會影像處理國際會議，2007，1：313-316。
[36] JIA H.，YIN Q. 和 LU M.採用區塊匹配域變換濾波和改進引導濾波的盲雜訊影像去雜訊。科學報告，2022年，12(1)，16195。https://doi.org/10.1038/s41598-022-20578-w
[37] PIRZADA M.、AMUR K.B.、ARAIN M.B. 與 MALOOKANI R.A. 用於影像去雜訊問題的影像驅動各向同性擴散率和互補正規化方法。速度快數學彙刊，2022年，10：1-13。https://doi.org/10.21015/vtm.v10i1.1186
[38] RUDIN L.I.、OSHER S. 和 FATEMI E. 基於非線性全變分的噪音消除演算法。物理學D：非線性現象，1992，60(1-4)：259-268。https://doi.org/10.1016/0167-2789(92)90242-F
[39] WEICKERT J. 影像處理中的各向異性擴散。卷。1.托伊布納，斯圖加特，1998年。http://www.lpi.tel.uva.es/muitic/pim/docus/anisotropic_diffusion.pdf
[40] PÖSCHL C. 吉洪諾夫 正則化與一般殘差項。博士論文。阿爾卑斯-亞得里亞海大學，2008。
[41] ESEDOGLU S.，和 OSHER S.J. 透過各向異性魯丁-奧舍-
法特米模型分解影像。純粹數學與應用數學通訊，2004，57(12)：1609-1626。https://doi.org/10.1002/cpa.20045
[42] PAPAFITSOROS K. 和 SCHÖNLIEB C.B. 用於影像重建的一階和二階組合變分方法。數學成像與視覺雜誌，2014，48：308-338。https://doi.org/10.1007/s10851-013-0445-4
[43] GELFAND I.M. 和 SILVERMAN R.A. 變分法。快遞公司，2000。https://thuvienso.hoasen.edu.vn/bitstream/handle/123456789/8961/Contents.pdf?sequence=3
[44] HÖLLIG K. 前向後向熱方程式存在無限多個解。美國數學會彙刊，1983，278(1)：299-316。https://www.ams.org/tran/1983-278-01/S0002-9947-1983-0697076-8/S0002-9947-1983-0697076-8.pdf
[45] WANG Z. 和 BOVIK A.C. 均方誤差：喜歡還是離開？訊號保真度測量的新視角。電機與電子工程師學會訊號處理雜誌，2009，26(1)：98-117。https://doi.org/10.1109/MSP.2008.930649
[46] BUADES A.、COLL B. 和 MOREL J.M. 一種影像去雜訊的非局部演算法。請參閱：2005年電機與電子工程師學會計算機學會計算機視覺和模式識別會議，美國加利福尼亞州聖地亞哥。2005年，2：60-65。https://doi.org/10.1109/CVPR.2005.38
[47] GRASMAIR M. 局部自適應全變分正則化，見：計算機視覺中的尺度空間和變分方法，第二屆國際會議，2009年，挪威沃斯，2009年，6月1-5日。2009年。http://dx.doi.org/10.1007/978-3-642-02256-2_28
[48] AMUR K.B.、MEMON A.L. 和 QURESHI S. 有限元法基於電視去噪優化問題的近似。邁赫蘭大學工程與技術研究雜誌，2014, 33(1): 121-128。http://publications.muet.edu.pk/research_papers/pdf/pdf848.pdf